



Rational design of a diffractive homogenizer for a laser beam

SVETLANA RUDNAYA¹, DAVID MISEMER² and FADIL SANTOSA³

¹*Avant! Corporation, 46871 Bayside Parkway, Fremont, CA 94538, U.S.A.*

²*Software, Electronics, and Mechanical Systems Technology Center, 3M Company, St. Paul, MN 55144, U.S.A.*

³*Minnesota Center for Industrial Mathematics, School of Mathematics, University of Minnesota, Vincent Hall, Minneapolis, MN 55455, U.S.A.*

Received 18 June 2001; accepted in revised form 17 April 2002

Abstract. The problem of designing a diffractive optical element (DOE) that produces a uniform-intensity beam from a spatially variable source is considered. Under the thin-lens approximation, the DOE is fully characterized by a phase function. Fresnel approximation is used to simplify the relationship between the input amplitude, the phase function, and the image intensity. The case where the light source has partial coherence is considered. A simple design procedure based on a lenslet array is proposed. It is shown that under certain physical assumptions, this ‘engineering’ solution leads to an effective design capable of producing a uniform intensity from a time-varying, non-uniform source.

Key words: approximate method, design procedure, diffractive optics, optical homogenizer

1. Introduction

Lasers are currently used in many processes in which materials are manipulated, including ablation of polymers, cutting of both metals and non-metals, and annealing of semiconductors. In many applications the processes include not only changing the materials’ properties but patterning them as well. In most of the applications, uniformity of the laser intensity over the entire beam is extremely important. Unfortunately, excimer lasers, widely used in processing materials, rarely have beams with the uniformity necessary for many applications. Equally important, the beam profile shifts over time in unpredictable ways.

The goal of the work described in this paper is the design of an optical element that transforms the intensity profile of the laser to provide a beam with very uniform intensity over the area of the work in the plane of the material. Several additional requirements are imposed on the design that severely restrict the design options. Foremost among them is that the passive optical element maintain uniformity, even as the beam profile shifts with time. In addition, the element must be very efficient; that is, a high percentage of the beam energy must be delivered to the work space.

For reasons of high efficiency and low cost, a diffractive rather than a refractive solution is desired. Computer-generated holograms are diffractive optical elements (DOE) that permit very general changes in phase and amplitude of an incoming wave. By adjusting the local phase of the wave, it is possible to diffract the light into a given two-dimensional intensity pattern. The design problem is thus reduced to finding the phase function, $\phi(\xi, \eta)$, that creates the desired target intensity $I_T(x, y)$ in the image plane. The DOE responsible for the phase shifts is called a phase mask. Although it is now possible to create masks that adjust the

phase continuously, ones that alter the phase from $-\pi$ to π in 2 to 16 discrete steps are more common and inexpensive to fabricate.

An additional complication is the need to account for the incomplete or partial coherence of the laser beam. An extended light source consists of many atomic oscillators, which act as light emitters. The phase and amplitude of these emitters undergo random fluctuations. If the emitters are close enough to each other, the fluctuations will not be independent. However, even in a laser, the fluctuations will be independent or uncorrelated when the separation is sufficiently large. When the fluctuations between the two points are perfectly correlated, then we say the emitters are coherent and we observe interference between waves arising from the two emitters. When the fluctuations are independent, the difference between the phases of the two emitters is random and we observe no interference phenomena in the time-averaged intensity. In reality, the correlation between the phases decays gradually as the separation between the two emitters increases. We will demonstrate that this partial coherence has profound effects on the intensity generated by a DOE.

In this paper, we develop a computationally economical but rigorous theoretical approach for incorporating the effects of partial coherence into the design of DOEs and an engineering approach to the design of a homogenizer that is insensitive to drift in the beam profile. We verify the engineering design by the direct simulation of intensity distribution in the image plane. The remainder of the paper is divided into three sections. In the following section we describe the technical approaches used to solve the problem. These include both the theory and the engineering ideas. The next section describes numerical results for a specific design case. We conclude with a discussion and summary.

2. Technical approach

Two problems need to be addressed to fully explore the problem of a beam homogenizer. First, one needs to construct a transformation between the phase change $\phi(\xi, \eta)$ introduced to the wavefront $U(P')$ and the intensity $I(P)$ in the image plane. The transformation must include the effects of partial coherence of the input intensity. Second, one needs to determine the phase function that creates the proper target intensity.

Let $P(x, y, z)$ be a point on the image plane, and let $P(\xi, \eta, 0)$ be a point on the phase mask. For a fully coherent wavefront $U(P')$ in the plane of the phase mask, the electromagnetic field on the image plane $U(P)$ is given by the Kirchhoff formula [1, p. 41],

$$U(P) = \frac{z}{i\lambda} \iint U(P') \frac{e^{ikr}}{r^2} ds \quad (1)$$

where $r = |P'P|$ and $k = 2\pi/\lambda$. The intensity at the image plane is given by the square modulus of the field

$$I(P) = |U(P)|^2. \quad (2)$$

For z much greater than the extent of the aperture, we can use the Fresnel approximation, where r is approximated by

$$r \approx z \left[1 + \frac{1}{2} \left(\frac{x - \xi}{z} \right)^2 + \frac{1}{2} \left(\frac{y - \eta}{z} \right)^2 \right]. \quad (3)$$

Let $p(\xi, \eta) = U(P')e^{i\phi(\xi, \eta)}$. Combining (3) and (1), as shown in [1, p. 60], we have

$$U(x, y, z) = \frac{e^{ik\left(z + \frac{x^2+y^2}{2z}\right)}}{i\lambda z} \iint \left\{ p(\xi, \eta) e^{i\frac{k}{2z}(\xi^2+\eta^2)} \right\} e^{-i\frac{k}{z}(x\xi+y\eta)} d\xi d\eta, \quad (4)$$

which, aside from multiplicative factors, is the Fourier transform of a modified field

$$\tilde{p}(\xi, \eta) = p(\xi, \eta) e^{i\frac{k}{2z}(\xi^2+\eta^2)}.$$

If $\mathcal{F}[g]$ denotes the two-dimensional Fourier transform of a function g , then,

$$U(x, y, z) = \frac{e^{ik\left(z + \frac{x^2+y^2}{2z}\right)}}{i\lambda z} \mathcal{F}[\tilde{p}]\left(\frac{x}{\lambda z}, \frac{y}{\lambda z}\right), \quad (5)$$

and

$$I(x, y) = \frac{1}{(\lambda z)^2} \left| \mathcal{F}[\tilde{p}]\left(\frac{x}{\lambda z}, \frac{y}{\lambda z}\right) \right|^2. \quad (6)$$

The partial coherence of the laser beam is taken into account by use of the theory of Wolf [2]. When the effect is included, Equations (1) and (2) are modified, and the intensity in the image plane is determined by

$$I(P) = \frac{z^2}{\lambda^2} \iint ds'' \iint ds' U(P') e^{i\phi(\xi, \eta)} U^*(P'') e^{-i\phi(\xi', \eta')} \frac{e^{ik(r'-r'')}}{(r'r'')^2} \gamma(|P'P''|). \quad (7)$$

Here, both P' and P'' are points on the phase mask, and $r' = |PP'|$ and $r'' = |PP''|$. The coherence function $\gamma(r)$ is a symmetric nonnegative function of r such that $\gamma(0) = 1$. $\gamma(r) \equiv 1$ corresponds to the full coherence model, and (7) reduces to (1) and (2). In general, the partial coherence function goes to 0 as the separation between the points becomes large; that is, $\gamma(r) \rightarrow 0$ as $r \rightarrow \infty$.

When z , the distance from the plane of the aperture to image point, is much greater than the size of the aperture, we can again apply the Fresnel approximation. In that case, we can write the intensity as

$$I(x, y, z) = \frac{1}{(\lambda z)^2} \iint \iint \tilde{p}(\xi, \eta) \tilde{p}^*(\xi', \eta') e^{-i\frac{k}{z}(x(\xi-\xi') + y(\eta-\eta'))} \gamma(r) d\xi d\eta d\xi' d\eta', \quad (8)$$

where $r = \sqrt{(\xi - \xi')^2 + (\eta - \eta')^2}$. By a change of variables $\xi - \xi' = \xi''$ and $\eta - \eta' = \eta''$, it is possible to rewrite (8) as

$$I(x, y, z) = \frac{1}{(\lambda z)^2} \iint d\xi'' d\eta'' g(\xi'', \eta'') \gamma\left(\sqrt{\xi''^2 + \eta''^2}\right) e^{-i\frac{k}{z}(x\xi'' + y\eta'')}, \quad (9)$$

where

$$g(\xi'', \eta'') = \iint d\xi d\eta \tilde{p}(\xi, \eta) \tilde{p}^*(\xi - \xi'', \eta - \eta'').$$

Apart from trivial constants, the integral in (9) is the two-dimensional Fourier Transform of the product of g and γ ; therefore, we may use the convolution theorem to write

$$I(x, y, z) = \frac{1}{(\lambda z)^2} \mathcal{F}[g(\xi, \eta)]\left(\frac{x}{\lambda z}, \frac{y}{\lambda z}\right) * \frac{1}{(\lambda z)^2} \mathcal{F}[\gamma(\sqrt{\xi^2 + \eta^2})]\left(\frac{x}{\lambda z}, \frac{y}{\lambda z}\right), \quad (10)$$

where $*$ denotes convolution.

Equation (10) shows that the intensity generated by a partially coherent beam is simply related to the intensity from a fully coherent beam. Because we want to differentiate between the cases of full and partial coherence, we let I_{FC} denote the intensity from a fully coherent beam and I_{PC} denote that arising from a partially coherent beam. Since $\mathcal{F}[g] = |\mathcal{F}[\tilde{p}]|^2$, it follows that

$$I_{PC}(x, y, z) = \frac{1}{(\lambda z)^2} |\mathcal{F}[\tilde{p}]|^2 * \frac{1}{(\lambda z)^2} \mathcal{F} \left[\gamma \left(\sqrt{\xi^2 + \eta^2} \right) \right].$$

By identifying I_{FC} in (6), we obtain

$$I_{PC} = I_{FC} * G. \quad (11)$$

G is called the slit function and is proportional to the Fourier Transform of the coherence function. Note that if $\gamma \equiv 1$, then $G(x, y) = \delta(x, y)$ and $I_{PC} = I_{FC}$, as we expect. On the other hand, in general, G acts as a smoother of I_{FC} .

The advantage of Equation (11) is that it involves calculation of two double integrals of $O(2n^2)$ operations, while Equation (7) requires calculation of one four-dimensional integral of $O(n^4)$ operations. It also provides better insight into how partial coherence affects the intensity profile.

In spite of the simplicity of the relation in Equation (11), its use is limited. For example, given a target image I_T and a known slit function G , it is tempting to define a modified target image by the equation

$$\tilde{I}_T * G = I_T.$$

and attempt to solve by the standard deconvolution procedure $\mathcal{F}[\tilde{I}_T] \cdot \mathcal{F}[G] = \mathcal{F}[I_T]$. In most cases, the solution does not exist because $\mathcal{F}[G]$ decreases faster than $\mathcal{F}[I_T]$.

We have a complete solution to the first technical problem, namely, finding a transformation between the phase function and the intensity for the case of partial coherence. The second task is to find the phase function that generates a uniform intensity in the image plane given an arbitrary intensity function in the plane of the phase mask. The electromagnetic field in the plane of the phase mask, $U_0(\xi, \eta)$, can be written as

$$U_0(\xi, \eta) = A(\xi, \eta) e^{i\psi(\xi, \eta)}.$$

In the remainder of the paper, we will assume that the phase ψ is constant, independent of ξ and η . The target image that we seek is a uniform intensity within an area bounded by $|x| \leq T_x/2$ and $|y| \leq T_y/2$. Thus, we seek a phase function

$$\phi(x, y) : A(x, y) \rightarrow \text{rect} \left(\frac{x}{T_x} \right) \text{rect} \left(\frac{y}{T_y} \right).$$

Several approaches [3, 4, 5, 6] have been used to design phase masks, but all have dealt with optimizing the phase function for a fixed input amplitude. One option for designing our homogenizing diffractive element would be to generalize those methods to seek the optimal design under the condition of a variable amplitude. We chose a different approach, more ‘engineering’ than ‘analytical’, based on an existing refractive homogenizer consisting of an array of lenslets. Each lenslet images the portion of the beam impinging on it on the entire target. If the area of the lenslet is sufficiently small, the lens array creates a uniform average

intensity in the image plane. The design was extended to a diffractive homogenizer in [7]. The approach is to divide the aperture of dimensions $L \times W$ into $N \times N$ small subintervals of length $\ell = L/N$ and $w = W/N$. The phase mask within each small subinterval is designed to project a uniform field within that subinterval onto the entire image. If the subintervals are sufficiently small, so that the variation in amplitude is small, the intensity in the image plane will approach a uniform, average value.

The success of the design outlined in the previous paragraph depends on two hypotheses which we verify later either analytically or numerically. First, we assume that the interactions between sub-intervals can be neglected. In that case, the cumulative intensity from an entire mask can be approximated as a sum of intensities arising from different sub-elements. This is not true for the fully coherent beam since $|U_1 + U_2|^2 \neq |U_1|^2 + |U_2|^2$, but it may be a good approximation for beams with 'small' coherence lengths. The second requirement is that the amplitude is sufficiently uniform over the sub-element and the beam is sufficiently symmetric to create a uniform average in the image.

The design problem can be greatly simplified if the amplitude of the incident beam $A(\xi, \eta)$, and γ are separable functions of ξ and η and $I_T(x, y)$ is a separable function of x and y . When these conditions are met, the two-dimensional design problem can be reduced to two, independent one-dimensional problems:

$$\begin{aligned}\phi_x(x) : A_x(x) &\rightarrow \text{rect}\left(\frac{x}{T_x}\right), \\ \phi_y(y) : A_y(y) &\rightarrow \text{rect}\left(\frac{y}{T_y}\right),\end{aligned}$$

resulting in an overall phase function $\phi(\xi, \eta) = \phi_x(\xi) + \phi_y(\eta)$. A consequence of the condition is that p and \tilde{p} are also separable functions. In particular, $\tilde{p}(\xi, \eta) = \tilde{p}_x \tilde{p}_y$, where

$$\tilde{p}_x(\xi) = A_x(\xi)e^{i\tilde{\phi}_x(\xi)},$$

and

$$\tilde{\phi}_x(\xi) = \phi_x(\xi) + \frac{\pi\xi^2}{\lambda z}, \quad (12)$$

is a modified phase function. In the remainder of the current paper, we will assume that A , γ , and I satisfy the separability conditions; therefore, the remaining analysis is restricted to the one-dimensional case.

The analysis is also simplified because the solutions for the various sub-elements are not independent. Note that for the central sub-element, we must find the modified phase function determined by

$$\tilde{\phi}(\xi) : \text{rect}\left(\frac{\xi}{\ell}\right) \rightarrow U(x, z), \quad |U(x, z)|^2 = I_T(x, z).$$

For a sub-element shifted by a distance a from the origin, we may use the shift theorem to define a related problem:

$$\tilde{\phi}(\xi - a) : \text{rect}\left(\frac{\xi}{\ell}\right) \rightarrow U(x, z)e^{-i\frac{k}{z}a}, \quad \left|U(x, z)e^{-i\frac{k}{z}a}\right|^2 = I_T(x, z).$$

Table 1. Parameters in the numerical experiment.

Parameter	Description	Value
L	Aperture size	40mm
T	Target size	26mm
z	Target to image distance	1.4m
λ	Wavelength	0.248 μ m
N	Number of subintervals	10
d	Pixel size (on image plane)	2 μ m
h	Coherence length	100 μ m

Thus, it is sufficient to find the phase function for just the central element and replicate that phase profile for all other sub-elements. With this approach the design of $N \times N$ sub-elements is reduced to just two one-dimensional problems.

The final step in the analysis of the homogenizer design is computing the phase function of the central sub-element. To do this, we use a well-known method described in [3, 4, 8]. We will assume that the subelements are chosen sufficiently small, so that the amplitude A may be considered constant over the sub-element. In that case, we seek a phase function that transforms

$$\text{rect}\left(\frac{\xi}{\ell}\right) \rightarrow \sqrt{\frac{\ell}{T_x}} \text{rect}\left(\frac{x}{T_x}\right).$$

Applying the method outlined in [3], we find the desired *modified phase* in the *central element* is

$$\tilde{\phi}_0(\xi) = \frac{\pi}{\lambda z} \left(\frac{T_x}{\ell}\right) \xi^2,$$

and, from Equation (12), the actual phase

$$\phi_0(\xi) = \frac{\pi}{\lambda z} \left(\frac{T_x}{\ell} - 1\right) \xi^2.$$

3. Numerical results

We now illustrate the application of the design methodology discussed in the preceding section to a typical problem. The relevant parameters are shown in Table 1. In this case we image a 40×40 mm beam onto a 26×26 mm target. The beam aperture is divided into 10 sub-intervals to guarantee good homogenization. The size of a sub-element is 4×4 mm, and the aperture-to-image distance is 1.4m. It is clear that the Fresnel approximation is valid. We assume a Gaussian model for the coherence function; that is, $\gamma(x) = \exp(-\pi(r/h)^2)$. For the particular laser of interest, the manufacturer specifies a lateral coherence length of 100 μ m [9].

We will compare the results of a mask design with a continuous phase with masks with discrete numbers of levels. In all cases – even the ‘continuous’ design – the phase takes on a constant value within a pixel, which in the current study, is 2 μ m on a side. The phase profiles

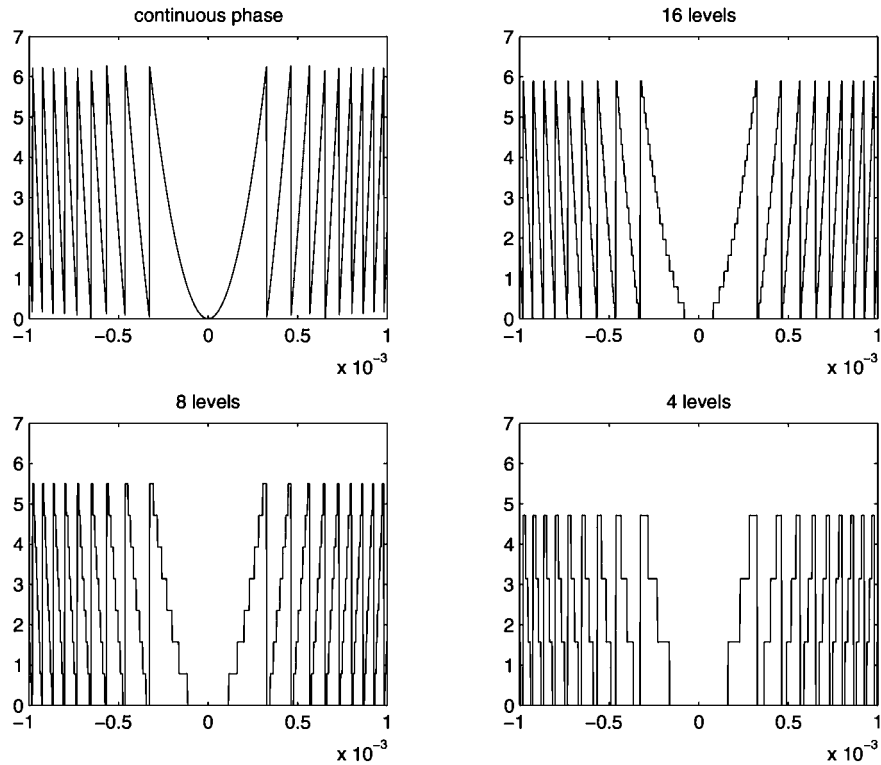


Figure 1. Parts of the quadratic phase and its discretizations.

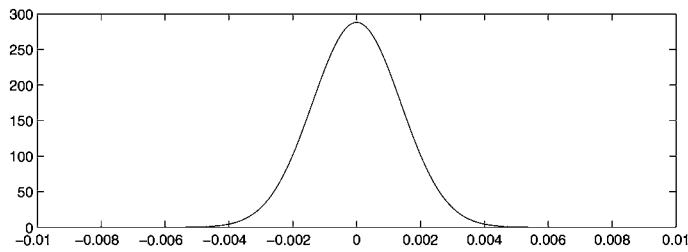


Figure 2. The slit function $G(x)$.

for the continuous and 4, 8, and 16 level phase functions are shown in Figure 1. The slit function is shown in Figure 2.

Our initial computations are performed for a single sub-element. The results are shown in Figure 3. The intensity profile for a fully coherent beam, determined by (6) for the phase profile shown in Figure 1, is shown on the left-hand side of the figure. The uniformity of the profile quickly degrades with decreasing number of levels in the phase function. The intensity profiles for a partially coherent beam, determined by (11), are shown on the left-hand side of the figure. Together, the figures clearly demonstrate the smoothing effects of partial coherence.

At this point we have explored only the case of a single sub-element. We now want to turn our attention to the cumulative effect of all of the sub-elements. The assumption in our engineering approach is that we can simply sum the intensities from all of the sub-elements. This assumption fails in the case of a fully coherent beam, but may be satisfied for a partially coherent laser.

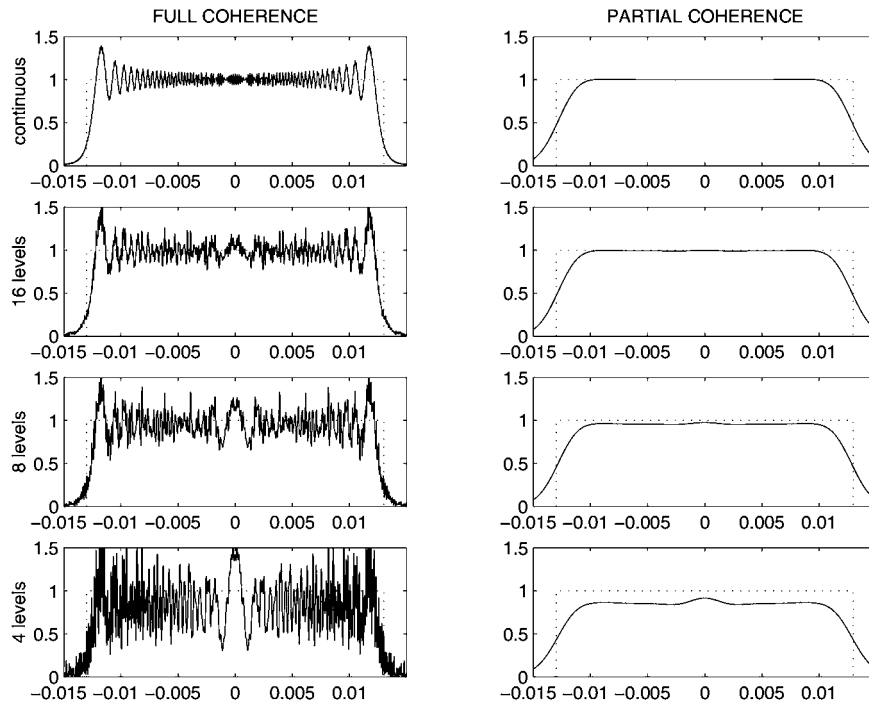


Figure 3. Intensity profiles compared with the target (shown in dashes).

We can estimate the effect of beam coherence on the profile by the following argument. Assume that $A(\xi) \approx A_j$ is approximately constant on the subinterval of length ℓ and at center a_j , $j = 1, \dots, N$. Let $U_0(x)$ and $I_0(x)$ represent the field amplitude and intensity on the image plane from the central sub-element. Then, by the shift theorem, the cumulative field is

$$U(x) = \sum_{j=1}^N A_j e^{-i \frac{kx a_j}{z}} U_0(x),$$

and the full coherence intensity is

$$I_{FC}(x) = \left| \sum_{j=1}^N A_j e^{-i \frac{kx a_j}{z}} \right|^2 \cdot |U_0(x)|^2 = R(x) I_0(x).$$

Since $R(x)$ is a highly oscillating function, $I_{FC}(x)$ will, in general, be very different from $I_0(x)$. Thus, the engineering approach will fail for very coherent laser beams.

On the other hand, for partial coherence, the technique may work well. We can estimate when it will. We may write

$$I_{PC}(x) = I_{FC} * G = (R I_0) * G.$$

If the sum over sub-elements is a good approximation, then it must be the case that

$$I_{PC}(x) = (R I_0) * G \approx \left[\sum_{j=1}^N A_j^2 \right] I_0 * G. \quad (13)$$

To see that this is plausible, we expand $R(x)$

$$R(x) = \left| \sum_{j=1}^N A_j e^{-i2\pi \frac{x a_j}{\lambda z}} \right|^2 = \sum_{j=1}^N A_j^2 + \sum_{j \neq k} A_j A_k e^{i \frac{kx}{z} (a_j - a_k)}.$$

We need to estimate the effect of the second term on I_{PC} . Let us look at fixed j and k , and consider the contribution to I_{PC} from this term,

$$S_{jk} = A_j A_k \int e^{i \frac{kx}{z} (a_j - a_k)} I_0(x) G(x - y) dy. \quad (14)$$

Assume now that $I_0(x)$ is nearly homogeneous, and its target size, $[-T_x/2, T_x/2]$, is much larger than the width of the Gaussian $G(x)$. For x away from $\pm T_x/2$,

$$I_0(x) G(x - y) \approx K G(x - y),$$

where K is some constant. Therefore, we can rewrite (14) as

$$\begin{aligned} S_{jk} &\approx K A_j A_k e^{i \frac{kx}{z} (a_j - a_k)} \int e^{-i2\pi \frac{y}{\lambda z} (a_j - a_k)} G(y) dy \\ &= K A_j A_k e^{i \frac{kx}{z} (a_j - a_k)} \mathcal{F}[G] \left(\frac{a_j - a_k}{\lambda z} \right) \\ &= K A_j A_k e^{i \frac{kx}{z} (a_j - a_k)} \gamma(a_j - a_k). \end{aligned}$$

For $\gamma(r) = \exp(-\pi(r/h)^2)$, clearly, we have

$$|S_{jk}| \leq |A_j A_k| \exp \left[-\pi \left(\frac{L}{Nh} \right)^2 \right].$$

This estimate gives us the conditions for N and L by which we can ignore the contribution from S_{jk} , and conclude that (13) is justified. For the parameters in our example, the estimate $S_{jk} \approx 0$ is very well satisfied.

To complete our numerical studies, we compute the total intensity from all pixels without approximation. To provide a more demanding numerical test of the design we have offset the peak of the beam to simulate drift in the profile. The input intensity is shown in the top panel of Figure 4.

The results are shown in the lower two panels of Figure 4. The center panel shows the result for a perfectly coherent input. While the beam does image primarily within the target, the oscillations in the intensity are much more rapid and irregular than those arising from a single sub-element. This is easily seen by comparing the central panel of Figure 4 with the top left-hand panel of Figure 3. The computations are consistent with our analysis of the unwelcome effects of full coherence. When the computation is repeated for a partially coherent beam, the smooth, regular profile of a single sub-element is recaptured. In Figure 4, we note that the maximum intensity for the partially coherent source is much lower than that of the fully coherent source. However, this is a conservative system. We verify this fact by computing the area under the input intensity over the aperture, and those under the image intensity at the image plane. We found the areas to be equal.

4. Concluding remarks

We have investigated the effects of partial coherence on the design for a diffractive homogenizer for a laser beam, whose profile changes over time. In particular, we have found a

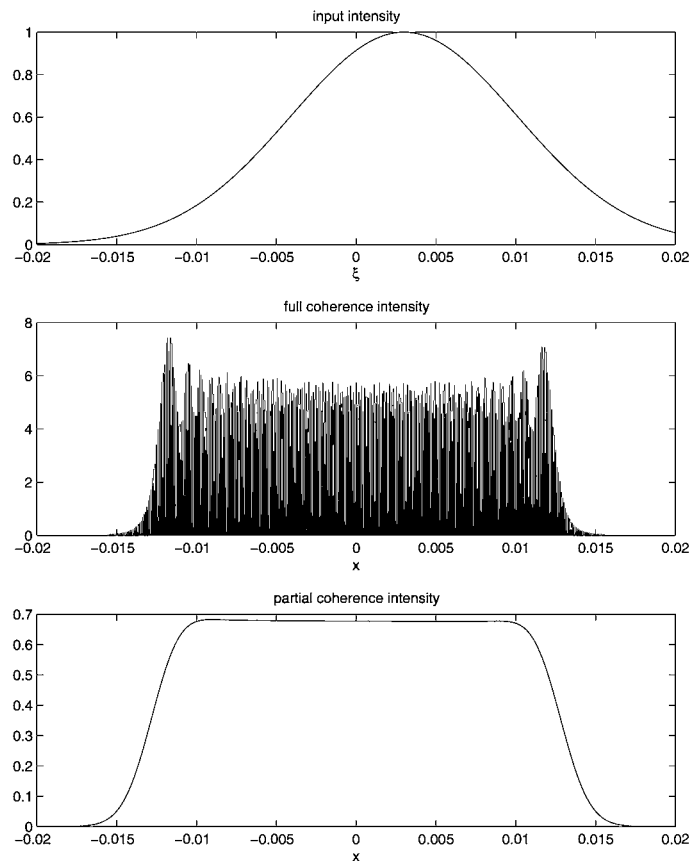


Figure 4. Top: input intensity. Center: full coherence intensity. Bottom: partial coherence intensity. Note the amplitude difference between full and partial coherence.

compact, computationally economical expression for the image intensity of a partially coherent beam in terms of intensity of the fully coherent beam and the Fourier Transform of the coherence function. We have used the result to study the intensity profile of a diffractive lenslet and the superposition of lenslet elements. Surprisingly, partial coherence is important obtaining the required uniformity with a phase function of fewer than 16 discrete steps.

To design our diffractive homogenizer, we used an engineering approach based on an analogy to refractive homogenizer, rather than an analytical approach. Although the design appears to work well, the efficiency of the phase mask can be quite low.

The main difficulty in this problem stems from the fact that the input intensity is time varying. We have addressed this issue by creating a design consisting of lenslets. It is not clear if this approach is very efficient. We are now considering an entirely different approach using stochastic optimization to take into account the fluctuating input profile. In arriving at the present design, we made an assumption that the coherence function and the phase functions are separable. An approach where this assumptions is removed needs to be developed.

ACKNOWLEDGEMENT

Svetlana Rudnaya gratefully acknowledges support from 3M. The authors acknowledge useful discussions with Dr. P. Fleming and Dr. R. Guenther. This research was supported in part by AFOSR through a MURI grant to the University of Delaware and by 3M Corporation.

References

1. J. W. Goodman, *Introduction to Fourier Optics*. New York: McGraw-Hill (1968) 287 pp.
2. M. Born and E. Wolf, *Principles of Optics*. New York: Pergamon Press (1964) 803 pp.
3. T. Dresel, M. Beyerlein and J. Schwinder, Design of computer-generated beam-shaping holograms by iterative finite-element mesh adaption. *Appl. Optics* 35 (1996) 6865–6874.
4. C. C. Aleksoff, K. K. Ellis and B. D. Neagle, Holographic conversion of a Gaussian beam to a near-filed uniform beam. *Optical Eng.* 30 (1991) 537–543.
5. F. Wyrowski and O. Bryngdahl, Iterative Fourier-transform algorithm applied to computer holography. *J. Optical Soc. America A*, 5 (1988) 1058–1065.
6. J. R. Fienup, Iterative method applied to image reconstruction and to computer-generated holograms. *Optical Eng.* 19 (1980) 297–305.
7. R. L. Guenther and C. L. Shoemaker, *Diffractive Homogenizer with Compensation for Spatial Coherence*. US Patent 6072631 (6 Jun 2000) and WO 0003286 A1 (20 Jan 2000).
8. N. C. Roberts, Beam shaping by holographic filters. *Appl. Optics* 28 (1989) 31–32.
9. P. Fleming, private communication.